J Biol Chem. Author manuscript; available in PMC 2011 August 18.

Published in final edited form as:
J Biol Chem. 2003 April 11; 278(15): 13133–13142. doi:10.1074/jbc.M300369200.

Characterization of Human Thioredoxin-like 2:

A NOVEL MICROTUBULE-BINDING THIOREDOXIN EXPRESSED PREDOMINANTLY IN THE CILIA OF LUNG AIRWAY EPITHELIUM AND SPERMATID MANCHETTE AND AXONEME*,S

Christine M. Sadek[‡], **Alberto Jiménez**[‡], **Anastasios E. Damdimopoulos**[‡], **Thomas Kieselbach**[§], **Magnus Nord**[¶], **Jan-Åke Gustafsson**[‡,¶], **Giannis Spyrou**[‡], **Elaine C. Davis**[‖], **Richard Oko**[**], **Frans A. van der Hoorn**[‡‡], and **Antonio Miranda-Vizuete**[‡,§§]

[‡]Center for Biotechnology, Protein Analysis Unit, Department of Biosciences at NOVUM, Karolinska Institutet, Huddinge S-14157, Sweden

[§]Center for Structural Biology, Protein Analysis Unit, Department of Biosciences at NOVUM, Karolinska Institutet, Huddinge S-14157, Sweden

[¶]Department of Medical Nutrition, Karolinska Institutet, Huddinge S-14157, Sweden

[‖]Department of Anatomy and Cell Biology, McGill University, Montreal, Quebec H3A 2B2, Canada

[**]Department of Anatomy and Cell Biology, Queen's University, Kingston, Ontario K7L 3N6, Canada

[‡‡]Department of Biochemistry and Molecular Biology, University of Calgary, Calgary, Alberta T2N 4N1, Canada

Abstract

We describe here the cloning and characterization of a novel member of the thioredoxin family, thioredoxin-like protein 2 (Txl-2). The Txl-2 open reading frame codes for a protein of 330 amino acids consisting of two distinct domains: an N-terminal domain typical of thioredoxins and a C-terminal domain belonging to the nucleoside-diphosphate kinase family, separated by a small interface domain. The Txl-2 gene spans ~28 kb, is organized into 11 exons, and maps at locus 3q22.3-q23. A splicing variant lacking exon 5 (Δ5Txl-2) has also been isolated. By quantitative real time PCR we demonstrate that Txl-2 mRNA is ubiquitously expressed, with testis and lung having the highest levels of expression. Unexpectedly, light and electron microscopy analyses show that the protein is associated with microtubular structures such as lung airway epithelium cilia and the manchette and axoneme of spermatids. Using *in vitro* translated proteins, we demonstrate that full-length Txl-2 weakly associates with microtubules. In contrast, Δ5Txl-2 specifically binds with very high affinity brain microtubule preparations containing microtubule-

*This work was supported by Swedish Medical Research Council Grants 03P-14096-01A, 03X-14041-01A, and 13X-10370, the Åke Wibergs Stiftelse, and the Karolinska Institutet to (A. M.-V.), by the Fundación Margit y Folke Pehrzon (to A. J.), and by grants from the Canadian Institutes of Health Research (to F. A. v. d. H. and R. O.).

S The on-line version of this article (available at http://www.jbc.org) contains Table 1.

§§To whom correspondence should be addressed: Center for Biotechnology, Dept. of Biosciences at NOVUM, Karolinska Institutet, Halsovagen 7, Huddinge S-14157, Sweden. Tel.: 46-8-608-3338; Fax: 46-8-774-5538; anmi@biosci.ki.se.

The nucleotide sequence(s) reported in this paper has been submitted to the GenBank™/EBI Data Bank with accession number(s) AF196568.

binding proteins. Importantly, Δ5Txl-2 also binds to pure microtubules, proving that it possesses intrinsic micro-tubule binding capability. Taken together, Δ5Txl-2 is the first thioredoxin reported to bind microtubules and might therefore be a novel regulator of microtubule physiology.

Thioredoxin (Trx)[1] is a small ubiquitous protein (12 kDa) that is conserved in all organisms from lower prokaryotes to human and functions as a general protein-disulfide reductase. The redox activity of thioredoxin resides in the sequence of its conserved active site Cys-Gly-Pro-Cys (CGPC), which undergoes reversible oxidation of the two cysteine residues from a dithiol to a disulfide form (1). Thioredoxin is maintained in its active reduced form by the flavoenzyme thioredoxin reductase, a selenocysteine-containing protein that uses the reducing power of NADPH (1). Several functions have been assigned to thioredoxin, mostly dependent on its redox activity, including regulation of transcription factor DNA binding activity, anti-oxidant defense, modulation of apoptosis, and the immune response (2). Moreover, abnormal thioredoxin expression has been correlated with a number of pathological situations such as cancer and Alzheimer's and Parkinson's diseases (3). The three-dimensional structure of thioredoxin is conserved through evolution and consists of five central stranded β-sheets externally surrounded by four α-helices (4). The active site is located in a protrusion of the protein between the β2-strand and the α2-helix (4). The conserved active site sequence and the three-dimensional structure of thioredoxin are the hallmarks of the thioredoxin family.

During recent years, the number of thioredoxin family members has increased substantially. Based on protein sequence organization, two distinct groups of thioredoxins can be distinguished. Group I includes those proteins that exclusively encode a thioredoxin domain; Group II is composed of fusion proteins of thioredoxin domains plus additional domains. Among those belonging to Group I are *Escherichia coli* Trx-1 (5), the three yeast thioredoxins (6, 7), and mammalian Trx-1 and Trx-2 (8, 9). Examples of Group II thioredoxins are *E. coli* Trx-2 (10), *Chlamydomonas* DLC14 and DLC15 proteins (11), mammalian Txl-1, and the spermatid-specific thioredoxins Sptrx-1 and Sptrx-2 (12–14). Until our discovery of Txl-2, Sptrx-2 was the only mammalian member of the family where two different known protein domains are present in the same polypeptide, as Sptrx-2 is a fusion protein of an N-terminal thioredoxin domain followed by three nucleoside-diphosphate (NDP) kinase domains. A similar domain structure is also found in sea urchin axonemal protein IC1 (15).

NDP kinases (also known as nm23) constitute another well known family of structurally and functionally conserved proteins identified across a wide range of species from bacteria to human. NDP kinases catalyze the transfer of γ-phosphates between nucleosides and deoxynucleoside di- and triphosphates, playing a pivotal role in maintaining a balanced pool of nucleotides (16, 17). In addition to the kinase function, nm23 proteins have been implicated in cell growth, cancer progression, and development (17, 18). Similar to

[1]The abbreviations used are: Trx, thioredoxin; AMP-PNP, adenosine 5′-(β,γ-imino)triphosphate; DTT, dithiothreitol; GAPDH, glyceraldehyde-3-phosphate dehydrogenase; GST, glutathione *S*-transferase; MALDI-TOF, matrix-assisted laser desorption ionization time-of-flight; MT, microtubule; NDP kinase, nucleoside-diphosphate kinase; ORF, open reading frame; PCD, primary ciliary dyskinesia; RACE, rapid amplification of cDNA ends; RCC1, regulator of chromosome condensation-1; Sptrx, spermatid-specific thioredoxin; Txl-2, thioredoxin-like protein 2; Δ5Txl-2, splicing variant lacking exon 5; UTR, untranslated region.

thioredoxins, humans have several NDP kinases (termed nm23-H1 to H8, of which nm23-H8 is also known as Sptrx-2). NDP kinases can also be classified into two groups based on sequence alignment and phylogenetic analysis (19). Group I is composed of nm23-H1 to H4 which all share a similar genomic organization consisting of a hexameric three-dimensional structure and the classical enzymatic activity of NDP kinases. Group II encompasses nm23-H5 to H8 genes, which are defined by a more divergent sequence, including a sequence of the active site which is not strictly conserved. Furthermore, nm23-H5, H7, and H8 have been shown to have a tissue-specific distribution mainly in testis/spermatozoa (14, 20, 21).

We report here the characterization of a novel human fusion protein composed of an N-terminal thioredoxin domain followed by an NDP kinase domain, named Txl-2. Based on the considerations above, Txl-2 should be classified as a member of the Group II of both thioredoxin and nm23 family of proteins. Txl-2 shares clear homology with Sptrx-2 with the difference that the latter has three NDP kinase domains following the thioredoxin domain. In accordance with nm23 nomenclature, Txl-2 should also be denoted as nm23-H9.

MATERIALS AND METHODS

cDNA Cloning of Human Txl-2 Gene

The Basic Local Alignment Search Tool (BLAST) (22) was used to perform a survey of different data bases at the National Center for Biotechnology Information (www.ncbi.nlm.nih.gov/) to identify new entries encoding potential novel members of the thioredoxin family. Using the thioredoxin domain of human Sptrx-2 as bait (14), we found the expressed sequence tag entry AI341589 to encode a putative thioredoxin-like sequence. Based on this sequence, the nested forward primers F1 (5′-GGGCAGCAGGAAGAAG-GATATTGC-3′) and F2 (5′-CAGGTCAACATCAGCACACAACAGC-3′) were used for 3′-RACE on a human testis cDNA library (Clontech, Palo Alto, CA). Based on the sequence obtained, the nested forward primers R1 (5′-CACCAGCCTAGATAGACATCAACAAC-3′) and R2 (5′-CTC-GATCCTCATCTTCTGGAAGAG-3′) were used for 5′-RACE in the same library. The resulting sequences were used to amplify by PCR the full-length and Δ5Txl-2 cDNA of human Txl-2 from the same library. The amplification products were cloned in the pGEM-Teasy vector (Promega) and sequenced in both directions.

Quantitative Real Time PCR

Human cDNA multiple tissue cDNA panels were purchased from Clontech, oligonucleotide primers were purchased from Cybergene AB (Stockholm, Sweden), and TaqMan probes and GAPDH kits were purchased from PE Applied Biosystems (Warrington, UK). To detect total Txl-2 mRNA, the forward primer was 5′-GGGCAGCAGGAAGAAGGAA-3′ (nucleotides 30–48), the reverse primer was 5′-TTAGTCCTTTGGAACTGAGCATTTC-3′ (nucleotides 115–91), and the Txl-2 TaqMan probe was 5′-CCTGCAGGTCAACAT-CAGCACCCA-3′ (nucleotides 54–77). To detect only full-length Txl-2 selectively, the forward primer was 5′-TCGTCTTGATGTCCTCGAAA-AGTAC-3′ (nucleotides 234–258), the reverse primer was 5′-CCTCTA-ACCACAGCCACCAGTT-3′ (nucleotides 323–302), and the Txl-2 long TaqMan probe was 5′-GAGCCAACCTTTCTGTTTTATGCAGGAGG-AG-3′ (nucleotides 189–212). All TaqMan probes were fluorescein labeled with the reporter dye FAM and

quencher dye TAMRA. All primer/probe sets were designed to cross an exon-intron boundary to prevent detection of genomic DNA. 90 μl of Mastermix containing 400 nM primers, 400 nM TaqMan probe, and 1× TaqMan Universal Mastermix (PE Applied Biosystems) was added to 1.8 μl of cDNA before aliquoting in triplicate to a 96-well microtiter plate. The cDNA was amplified using an ABI PRISM 7700 thermocycler (PE Applied Biosystems) under the following conditions: 1 cycle at 50 °C for 2 min and 95 °C for 10 min followed by 40 cycles at 95 °C for 15 s and 60 °C for 1 min. The amounts of GAPDH and Txl-2 mRNA were calculated using the standard curve method (separate tubes, following the instructions in User Bulletin 2; PE Applied Biosystems). Fluorescence intensity was measured during the PCR run. A graph was drawn with the threshold cycle *C*T value *versus* the logarithm of the amount of serially diluted control cDNA. Using this graph and the *C*T value of GAPDH and transforming acidic coiled-coil samples, the relative amount of TACC mRNA adjusted for GAPDH was calculated. All real time PCR experiments were carried out in triplicate and performed a minimum of three independent times with similar results.

To determine the relative amounts of full-length and alternatively spliced Δ5Txl-2 in samples, plasmids containing either form were quantified and serially diluted to prepare standard curves for analysis at the same time as sample tissue cDNA. As a secondary control, samples were also prepared containing various mixtures of Txl-2 full-length and Δ5Txl-2 plasmids. Each sample was amplified using the Txl-2 primer and probe sets to determine the quantity of either total or full-length Txl-2.

Expression and Purification of Human Txl-2

The ORF encoding human Txl-2 was cloned into the *Bam*HI-*Eco*RI sites of the pGEX-4T-1 expression vector (Amersham Biosciences) and used to transform *E. coli* BL21(DE3). A single positive colony was inoculated in 1 liter of LB medium plus ampicillin and grown at 37 °C until A_{600} = 0.5. The production of the fusion protein was induced by the addition of 0.5 mM isopropyl-1-thio-β-D-galactopyranoside, and growth was continued for another 3.5 h. Overexpressing cells were harvested by centrifugation and frozen until use. The cell pellet was resuspended in 40 ml of 20 mM Tris-HCl, 1 mM EDTA, and 150 mM NaCl plus protease inhibitor mixture at the concentration recommended by manufacturer (Sigma). Lysozyme was added to a final concentration of 0.5 mg/ml with stirring for 30 min on ice. 1% sarkosyl was added, cells were disrupted by a 10-min sonication, and the supernatant was cleared by centrifugation at 15,000 × *g* for 30 min and loaded onto a glutathione-Sepharose 4B column (Amersham Biosciences). Binding to the matrix was allowed to occur for 2 h at room temperature. Thrombin (5 units/mg of fusion protein) was used to remove glutathione *S*-transferase by incubation overnight at 4 °C. The resulting protein preparation was then subjected to ion exchange chromatography using a HiTrap Q column (Amersham Biosciences), and human Txl-2 was eluted using a gradient of NaCl. For gel filtration chromatography, the Txl-2 preparation from ion exchange chromatography was applied to a Superdex G-75 preparation grade column (Amersham Biosciences) under nondenaturing conditions, pre-equilibrated with the same buffer as the protein preparation. Protein concentration was determined from the absorbance at 280 nm using a molar extinction coefficient of 24,310 M^{-1} cm^{-1}, calculated with the Protean Program included in the

DNASTAR Software Package (DNASTAR Inc., Madison, WI). An identical protocol was used to purify the recombinant Δ5Trx-2 variant, and the protein concentration was determined using the same molar extinction coefficient as that of the full-length form.

Mass Spectrometry Analysis

Reduced Txl-2 was prepared by incubation in the presence of 250 mM DTT on ice for 30 min, and unreduced controls were treated under identical conditions but in the absence of DTT. The samples were diluted 10 times with 0.1% (v/v) trifluoroacetic acid and mixed with an equal volume of a saturated solution of sinapinic acid in 33% (v/v) acetonitrile and 0.1% (v/v) trifluoroacetic acid. An aliquot of 0.5 μl of this mixture was crystallized on a microcrystalline layer that had been prepared with a saturated solution of sinapinic acid (Fluka) in ethanol (23). The spectra were acquired using a Reflex III mass spectrometer from Bruker (Germany) and calibrated using the high mass protein standard from Aglient Technologies which contained 66,430.2-Da bovine serum albumin, 16,951.5-Da equine cardiac myoglobin, and 12,359.2-Da equine cardiac cytochrome *c*. Data processing and evaluation were carried out with the XMASS software from Bruker.

Antibody Production

Purified GST-hTxl-2 was used to immunize rabbits (Zeneca Research Biochemicals). After six immunizations, serum from rabbits was purified by ammonium sulfate precipitation. Affinity-purified antibodies were prepared using a cyanogen bromide-activated Sepharose 4B column, onto which 0.5 mg of recombinant Txl-2 fragment had been coupled using the procedure recommended by the manufacturer (Amersham Biosciences). The specificity of the antibodies was tested by Western blotting using recombinant and *in vitro* translated human Txl-2 and Δ5Txl-2. Immunodetection was performed with horseradish peroxidase-conjugated donkey anti-rabbit IgG diluted 1/5,000 following the ECL protocol (Amersham Biosciences).

Mouse/Rat Testis and Epididymis Sample Preparation, Immunocytochemistry, and Electron Microscopy

Adult male Sprague-Dawley rats and CD mice were anesthetized, and testes and epididymes were fixed by perfusion through the abdominal aorta and heart, respectively, either with 0.5% glutaraldehyde and 4% paraformaldehyde in 0.1 M phosphate buffer containing 50 mM lysine, pH 7.4, or with 4% paraformaldehyde (mice only) or in Bouin's fixative (for light microscopy). Tissues destined for Lowicryl (SPI Supplies, West Chester, PA) embedding (for electron microscopy) were immersed in the respective fixatives for 2 h at 4 °C, washed three times in phosphate buffer, and incubated with phosphate buffer containing 50 mM NH_4Cl for 1 h at 4 °C. Tissues were subsequently washed in buffer, dehydrated in graded methanol up to 90%, and infiltrated and embedded in Lowicryl K4M. Thin sections were mounted on Formvar nickel-coated grids for immunogold labeling. Bouin's fixed rat and human tissue were washed extensively in 75% alcohol before being completely dehydrated in ethanol and embedded in paraffin. Paraformaldehyde-fixed tissue were washed in phosphate buffer, dehydrated, and embedded in paraffin.

For light microscopic immunocytochemistry, 5-μm paraffin sections were deparaffinized and hydrated through a graded series of ethanol concentrations before immunoperoxidase localization with anti-Txl-2 antibody by standard procedures (24). For electron microscopic immunocytochemistry ultrathin Lowicryl sections on Formvar nickel-coated grids were immunogold labeled according to the procedure of Oko *et al.* (25). Staging of the cycle of the seminiferous epithelium and determining the steps of spermiogenesis were done according to the classifications of Leblond and Clermont (26).

Mouse Lung Sample Preparation, Immunocytochemistry, and Electron Microscopy

Adult C57BL/6 mice were were killed by cervical dislocation, the trachea was cannulated, and the cannula was tied firmly in place. The anterior chest wall was removed and the lungs dissected out. The lungs were infused via the tracheal cannula with 4% paraformaldehyde, pH 7.4, at 20 cm H_2O pressure and maintained at this pressure for 5 min. The lungs were subsequently kept in fixative overnight at 4 °C. After fixation the lungs were dehydrated through a graded series of ethanol. Finally the lobes were separated and placed into individual cassettes and embedded in paraffin. The central portions of the blocks were sectioned at 5-μm intervals, and the sections were mounted on glass slides, deparaffinized, and hydrated before immunoperoxidase localization with anti-Txl-2 antibody. To block unspecific binding of secondary antibodies, sections were incubated in blocking solution (5% normal goat serum). Primary antibody was added at a 1/20 dilution in blocking solution, and in control experiments 0.03 mg/ml blocking peptide was included. After several washes, the Vectastain-ABC kit (Vector Laboratories, OH) was used for visualization. Sections were slightly counterstained with Mayer's hematoxylin, dehydrated, and mounted.

Indirect immunogold labeling was used at the electron microscope level to localize Txl-2 specifically. Small pieces (1 mm^3) of adult mouse lung were fixed in 4% paraformaldehyde in 0.1 M Sorensen's buffer, pH 7.4, for 4 h at 4 °C. After washing in several changes of Sorensen's buffer at 4 °C, the tissues were dehydrated in a graded series of methanol at progressively lower temperatures to −20 °C. The tissue pieces were then infiltrated and embedded in Lowicryl K4M at −35 °C. Lowicryl blocks were polymerized by ultraviolet illumination for 24 h at − 35 °C and an additional 48 h at −10 °C.

Lowicryl thin sections were placed on Formvar nickel-coated grids and incubated face-down on drops of blocking solution consisting of 1% bovine serum albumin in 50 mM Tris, pH 7.6, with 100 mM sodium chloride. After 30 min, the grids were transferred to drops of primary antibody diluted 1:10 in blocking solution and left overnight in a humidity chamber at 4 °C. The following day, the grids were washed face-down on wells containing 50 mM Tris, pH 7.6, with 100 mM sodium chloride for 3 × 10 min. The grids were then incubated on blocking solution for an additional 30 min prior to being transferred to drops of secondary antibody (goat $F(ab')_2$ anti-rabbit IgG conjugated to 10 nm of colloidal gold; Ted Pella) diluted 1/30 in blocking solution. After 1 h, the grids were washed as described previously and then rinsed in distilled water. Immunolabeled sections were counterstained with methanolic uranyl acetate followed by lead citrate.

Microtubule (MT) Binding Assay

MTs were purified from rat and mouse brain essentially as described previously (27), resulting in MT preparations that contain MTs and MT-binding proteins including mitogen-activated proteins and kinesins. In short, brain samples were extracted in ice-cold BRB80 buffer containing protease inhibitors pepstatin, leupeptin, and phenylmethylsulfonyl fluoride and centrifuged at 55,000 rpm for 15 min at 4 °C. Supernatants containing depolymerized MTs were removed and stored on ice. MT extracts were next supplemented with 0.5 mM GTP, 15 units/ml hexokinase, and 20 mM D-glucose to deplete ATP. Next the extracts were warmed to 30 °C and 5 μM paclitaxel was added. After a 5-min incubation at 30 °C, 15 μM Taxol was added (20 μM total). 2 mM AMP-PNP was added to stabilize kinesin heavy chains on MTs. The extracts were layered onto sucrose cushions and spun at 40,000 rpm for 20 min at 22 °C. The cushion was washed twice with BRB80 before being removed to avoid contamination of the MT pellets. MT pellets were resuspended in 100 μl of BRB80 and depolymerized on ice for 20 min. 0.5 mM GTP and 2 mM AMP-PNP were added to the MT preparations. Extracts were warmed to 30 °C and polymerized and centrifuged as above. MT pellets were subjected to another round of depolymerization and polymerization as above. Final pellets of polymerized MTs were resuspended in 10% glycerol and BRB80 and flash frozen in liquid nitrogen.

Pure polymerized MTs were made from purified tubulin (CytoSkeleton Inc.) as follows: 10 μl of pure tubulin (10 mg/ml) was mixed in BRB80 buffer with 5 μl of glycerol and 3.3 μl of 0.15 mM paclitaxel, and water was added to 50 μl. This reaction was incubated at 33 °C for 15 min. The mix was loaded on a glycerol cushion of equal volume and spun at 22,000 rpm for 30 min at room temperature. The MT pellet was recovered and dissolved in 50 μl of BRB80 buffer and 10% glycerol.

To analyze binding of Txl-2 and Δ5Txl-2 to MT, both forms were transcribed and translated *in vitro* in the presence of [^{35}S]cysteine using the TNT reticulocyte transcription and translation system (Pro-mega). Radiolabeled proteins were incubated with polymerized brain MTs or with pure MTs at 30 °C for 15 min in the presence of 2 mM AMP-PNP, 0.5 mM GTP, and 20 μM paclitaxel. MTs were pelleted at 30,000 rpm for 15 min at 22 °C. Supernatants were saved for SDS-PAGE analysis. Two subsequent pelleting reactions were performed. Aliquots of both supernatants and final pellets were boiled in SDS sample buffer and analyzed by electrophoresis on 10% SDS-polyacryl-amide gels. The gels dried and exposed to KODAK BIOMAX film. Intensity of bands was quantitated by image analysis. In the indicated experiments MTs were preincubated with anti-Txl-2 antibodies or with human recombinant Txl-2.

RESULTS

cDNA Cloning, Sequence Analysis, Genomic Organization, and Chromosomal Localization of the Human Txl-2 Gene

By sequence comparison with human Trx-1 (8), we found that GenBank expressed sequence tag entry AI341589 (from pooled germ cell tumors) encoded a putative novel human Trx-like sequence. Therefore, we designed specific primers based on the AI341589 sequence and

performed 5′- and 3′-RACE PCR analysis using a human testis cDNA library to clone the full-length cDNA sequence of this novel protein. The complete sequence of the cDNA obtained consists of an ORF of 990 bp, a 5′-UTR of 27 bp, and a 3′-UTR of 432 bp upstream of the poly(A)$^+$ tail (Fig. 1*A*). In addition, the PCR also rendered a smaller band, which corresponded to a putative splicing variant (see below). Human Txl-2 ORF encodes a protein of 330 amino acids with a calculated molecular mass of 36.9 kDa and a pI of 4.73. Analysis of the human Txl-2 sequence identified two distinct domains: an N-terminal domain (comprising the first 105 residues) similar to thioredoxins and a C-terminal domain composed of one NDP kinase domain (Fig. 1*B*). The domains are separated by a small interface domain. The Txl-2 protein domain organization resembles that of Sptrx-2 (14), with the exception that Sptrx-2 has three NDP kinase domains. Regarding the N-terminal thioredoxin domain, some of the structural amino acids that are conserved in previously characterized mammalian thioredoxins (including Sptrx-2) such as Asp-26, Trp-31, Pro-75, or Gly-91 (numbers refer to those of human Trx-1) are also conserved in Txl-2. However, other residues shown to be essential for catalysis, maintenance of three-dimensional structure, or protein-protein interactions are substituted, for instance Phe-11, Ala-29, Pro-40, Asp-58, or Lys-81 (4) (see Fig. 2*B* of Ref. 14).

Additionally, the Txl-2 C-terminal domain consists of one NDP kinase domain. Following the nomenclature for NDP kinase protein family, Txl-2 should be considered the ninth member of this family and therefore termed nm23-H9 (19). A protein alignment and phylogenetic analysis of all human NDP kinase domains show that Txl-2 belongs to NDP kinase Group II (Fig. 2, *A* and *B*) (19). The protein alignment of the Txl-2 domain with all of the previously identified thioredoxin proteins has been reported elsewhere (14). The 3′-UTR of human Txl-2 mRNA contains a short interspersed repetitive element of the Alu family spanning from base 1156 to 1439 (Fig. 1*A*). This is not the first report of the presence of such a repetition in a member of the NDP kinase family as nm23-H6 mRNA also harbors an Alu sequence located in the 3′-UTR of its mRNA (21). Interestingly, both proteins are testis-specific. In x-ray crystallography and site-directed mutagenesis studies, nine residues essential for catalysis and stability of nm23 proteins have been identified (17, 19). Human Txl-2 has five of these nine conserved residues regarded as crucial for enzymatic activity (Fig. 2*A*). Furthermore, the sequence of the active site (NAVH) matches the consensus for this family of proteins (N*XX*H) where *X* can be any residue (Fig. 1, *A* and *B*).

A comparison of the protein sequence with PROSITE data base (28) identified, along with the above mentioned thioredoxin and NDP kinase domains, several potential phosphorylation sites and an RCC1 (regulator of chromosome condensation-1) signature present between residues 222 and 232 (Fig. 1*A*).

A homology search in the Human Genome Sequence Data Base (www.ncbi.nlm.nih.gov/genome/guide/human/) identified the Txl-2 genomic region to be localized to chromosome 3q22.3-q23 (entry NT_025664.5 Hs3_25820) (Fig. 3). Using the Genomatix Software (www.genomatix.de/) we have determined that the Txl-2 gene spans ~28 kb and is organized into 11 exons and 10 introns, all conforming to the GT/AG rule (see supplemental Table 1 in on-line version of this work). Analysis of the splicing variant that appeared during the cloning PCR indicated that it lacked exon 5.

Differential Expression Pattern of Txl-2 mRNA in Various Human Tissues

Initially, we used multiple tissue Northern blots to determine the size and tissue distribution of human Txl-2 mRNAs with either the ORF or the thioredoxin domain as probes. However, we were unable to detect any signal despite the use of low stringency conditions and extended time of exposure (data not shown). To improve the sensitivity of our studies and to provide a means of quantification, we therefore used real time PCR to determine Txl-2 mRNA levels in a variety of human adult tissues (Fig. 4*A*). Our results demonstrate that total Txl-2 mRNA in adult tissues is very low. However, highest levels are found in testis and lung, whereas lower levels are found in brain, thymus, spleen, prostate, kidney, and ovary. Txl-2 mRNA is virtually absent in colon, liver, and heart. We also determined the relative amounts of full-length Txl-2 *versus* alternatively spliced Δ5Txl-2 in the three tissues with highest mRNA content: testis, lung, and brain. As shown in Fig. 4*B*, Δ5Txl-2 is the predominant mRNA form in all three cases. In testis and lung the ratio of Δ5Txl-2 to Txl-2 is ~60:40, whereas in brain this ratio is clearly shifted to a much higher relative amount of the spliced variant, 90:10.

Expression and Enzymatic Activity of Human Txl-2 Protein

Recombinant human Txl-2 migrated at 36 kDa in good agreement with its theoretical size (Fig. 5*A*, *inset*). Members of the NDP kinase family have been described as having an oligomeric structure in their native conformations (19). To evaluate whether this was also the case for Txl-2, we performed gel filtration chromatography and found two peaks corresponding to the monomeric and the dimeric conformation, indicating that in its native form, Txl-2 might be found in equilibrium between both forms (Fig. 5*A*). Analysis of the fractions eluting from the column by SDS-PAGE ruled out the possibility of protein contamination or degradation as an explanation for the appearance of two peaks (data not shown). Next, we used MALDI-TOF mass spectrometry to determine whether the dimeric conformation is maintained by disulfide bonding. Fig. 5*B* shows Txl-2 spectra in which two peaks can be identified, corresponding to the monomeric and dimeric forms. Incubation of the Txl-2 protein with DTT buffer resulted in a decrease of the dimeric peak, further demonstrating that disulfide bonds are responsible, at least in part, for the dimeric conformation.

Enzymatic activity of thioredoxin is usually assayed by the capacity to reduce the disulfide bonds of insulin using either DTT as artificial reductant or NADPH and thioredoxin reductase as a more physiological reducing system (1). We were unable to detect any enzymatic activity in either enzymatic assay, using full-length Txl-2 or the Δ5Txl-2 variant (data not shown). We also determined whether Txl-2 behaves as dominant negative, competing with Trx-1 for binding to thioredoxin reductase. As shown in Fig. 5*C*, increasing amounts of full-length Txl-2 weakly, but consistently, compete with human Trx-1 in the thioredoxin reductase enzymatic assay, thus suggesting that the absence of enzymatic activity of Txl-2 is not the result of a lack of interaction with the reductase.

On the other hand, NDP kinases catalyze the transfer of a terminal phosphate residue from NTPs to NDPs according to a ping-pong mechanism. The first step of this reaction consists of the autophosphorylation of the enzyme at a conserved histidine of the active site (29, 30).

Txl-2 was unable to undergo autophosphorylation under the same experimental conditions that allowed positive control yeast NDP kinase autophosphorylation (31).[2]

Cellular and Subcellular Localization of Txl-2 Protein

As determined by real time PCR, testis and lung were the tissues with the highest amount of Txl-2 mRNA. We therefore selected these two tissues to address the cellular and subcellular localization of Txl-2 protein. Thioredoxins and NDP kinases display a high degree of amino acid identity between humans and rodents (www.ncbi.nlm.gov/LocusLink/). Because of sample availability and considering the identity between humans and rodents, we decided to perform immunohistochemical analysis on mouse and rat samples. As shown in Fig. 6, Txl-2 labeling is readily detected in the cilia of the mouse lung airway epithelium. Preincubation of the antibodies with human recombinant Txl-2 abolished the signal. Similarly, Fig. 7 demonstrates the presence of Txl-2 in rat testis seminiferous tubules, where the protein is associated with the spermatid tail and manchette, a microtubular structure assumed to participate in the elongation of the spermatid head and storage of proteins for later delivery to the developing tail (32). Again, antibody preadsorbed with the human recombinant protein gave no labeling, thus confirming the specificity of the antibodies and their cross-reactivity in rodent samples. Surprisingly, a strong and specific labeling in the testis blood vessels was also obtained. Identical results were obtained with mouse testis sections (data not shown).

The finding of Txl-2 protein in such specific cellular structures prompted us to investigate in more detail its subcellular localization because the possibility existed that Txl-2 is somehow associated with MTs. Surprisingly, by immunogold electron microscopy, we found Txl-2 in association with MTs both in lung and testis: the Txl-2 signal was over MTs that make up lung cilia as well as over the MT-containing spermatid manchette and axoneme (Figs. 8 and 9). In addition, in testis blood vessels Txl-2 colocalized with fibrillar components of smooth muscle tissue (Fig. 10).

MT Binding Activity of Human Txl-2

The immunolocalization data strongly suggested that Txl-2 might be able to bind MTs. This would constitute the first example of such a characteristic for thioredoxins. To prove this possibility, we performed *in vitro* MT binding assays using ^{35}S-labeled *in vitro* translated proteins. First, translated Txl-2 and Δ5Txl-2 proteins were analyzed for binding to brain MTs containing myelin basic proteins. As shown in Fig. 11*A*, *upper panel*, full-length Txl-2 binds only weakly to MTs in this assay as demonstrated by the presence of recombinant protein in both the MT pellet (*p; lane a*, *upper panel*) as well as in supernatant 2 (*s2; lane c*, *upper panel*), a consequence of release of Txl-2 from MTs during the course of the experiment. Preincubation of the *in vitro* translated Txl-2 either with specific antibodies or unlabeled recombinant protein did not result in a significant decrease of the binding (*lanes d* and *g*, *upper panel*, respectively). The appearance of two bands when the Txl-2 construct is translated *in vitro* is probably a consequence of the use of an internal methionine as translational start in the *in vitro* system (Fig. 1*A*). In agreement with the immunoelectron

[2]A. Karlsson, personal communication.

microscopy data, which suggested that Δ5Txl-2 protein can colocalize with MTs, Δ5Txl-2 protein is clearly present in the pellet fraction and not in the supernatant 2, demonstrating that Δ5Txl-2 is stably bound to MTs in this assay (Fig. 11*A*, *lower panel*). Moreover, the binding is specific because preincubation of Δ5Txl-2 with unlabeled recombinant protein or anti-Txl-2 antibodies decreases binding to 49 and 28%, respectively, of the levels achieved with the Δ5Txl-2 protein alone (*lanes d* and *g*, *lower panel*, respectively). Because brain MT preparations contain, in addition to MTs, MT-binding proteins such as mitogen-activated proteins and kinesins, these experiments demonstrate that Txl-2 associates with MTs but cannot distinguish direct from indirect MT binding. To distinguish these two mechanisms we compared MT binding for both Txl-2 and Δ5Txl-2 using pure MTs and brain MTs. The results are shown in Fig. 11*B*. The data show that Δ5Txl-2 binds with high affinity to pure MTs (*lane i*) with very little material in the second supernatant (*lane h*). There is no significant difference in Δ5Txl-2 MT binding using pure or brain MTs. This proves that Δ5Txl-2 MT binding is direct and establishes Δ5Txl-2 as the first genuine MT-binding thioredoxin. As with brain MTs, full-length Txl-2 associates significantly more weakly with pure or brain MTs (*lanes c* and *f*, respectively).

DISCUSSION

MTs are fibrous cytoskeletal components of the eukaryotic cell cytoplasm which serve to perform a wide variety of functions, such as cell motility and division, organelle transport, and morphogenesis. In addition, MTs are the main components of the complex and highly organized axonemal structures found in cilia and flagella (33). There is evidence that some members of the NDP kinase family associate with microtubular structures (34–38). In contrast, only four proteins containing a thioredoxin domain have been reported to be associated to microtubular structures and in all cases in lower eukaryotes: LC14 and LC15 proteins from *Chlamydomonas* flagellum (11) and the dynein intermediate filaments IC1 from sea urchin sperm axoneme and IC3 of the ascidian, *Ciona intestinalis* (15, 39). The last two proteins are composed of an N-terminal thioredoxin domain followed by three NDP kinase domains. Similar domain structure has been found in Sptrx-2 (14), a human protein exclusively expressed in the spermatozoon fibrous sheath, a structure that surrounds the axoneme and outer dense fibers of sperm tail principal piece.[3] However, Sptrx-2 is not likely to interact with sperm tail MTs despite the clear domain homology with the IC proteins because they are kept apart from each other by the outer dense fibers.

We report here a novel protein (Txl-2 and Δ5Txl-2, a splicing variant lacking exon 5) consisting of an N-terminal thioredoxin domain followed by one NDP kinase domain in close similarity to Sptrx-2 (14). Indeed, a phylogenetic analysis of the separate domains places both proteins in the same tree branch. However, a comparison of the expression pattern of both proteins shows important differences. Sptrx-2 is a testis-specific protein (14), whereas Txl-2 is more ubiquitous and has lower overall expression levels, although it is more abundant in testis and lung. Unexpectedly, an immunohistochemical analysis of Txl-2/Δ5Txl-2 expression in these two tissues shows the protein to be in close association with microtubular structures: cilia of the lung airway epithelium and the manchette and axoneme

[3]A. Miranda-Vizuete, K. Tsang, Y. Yu, A. Jiménez, M. Pelto-Huikko, P. Sutovsky, and R. Oko, unpublished results.

of the spermatids. Furthermore, Txl-2/Δ5Txl-2 is found within the fibrillar components of the testis blood vessel smooth muscle.

The electron microscopic study suggested that Txl-2 might represent the first MT-binding thioredoxin family member, which would have a considerable impact on its potential functions. This possibility was approached by *in vitro* MT binding assays. These experiments, using pure MTs, established definitively that Δ5Txl-2 could bind directly to MTs, without the aid of MT-associated proteins such as kinesins or mitogen-activated proteins. In contrast the full-length Txl-2 protein has a much reduced affinity for MT.

At this stage we do not know whether Txl-2, Δ5Txl-2, or both associate with MTs in lung and spermatids because the polyclonal antibodies raised against full-length Txl-2 recognize both forms. In light of the quantitative RT PCR data and the *in vitro* MT binding experiments, it appears most likely, however, that Δ5Txl-2 rather than Txl-2 is the major MT-binding form. The difference in affinity may be explained in two ways. First, the MT interacting area in Δ5Txl-2 may be disrupted by the presence of exon 5 in the Txl-2 form, or exon 5 sequences cause a change in Txl-2 conformation affecting MT binding. Further *in vitro* analysis of Δ5Txl-2 deletion mutants can address this point. Second, cell- or tissue-specific factors might be required to modulate the MT binding activity of Δ5Txl-2, which are not present in the *in vitro* MT binding assay. Analysis of brain may help to resolve this possibility because in that tissue Δ5Txl-2 is by far the major form. Be that as it may, our results demonstrate for the first time that genuine MT-binding members of the thioredoxin family exist.

At present we can only speculate on the mechanism of binding of Δ5Txl-2 to MTs and its role in MT physiology. Cysteine residues in tubulin are actively involved in regulating ligand interactions and MT formation both *in vivo* and *in vitro* (40). Because thioredoxins are considered to be general protein di-sulfide reductases, it is conceivable that the cysteine residues at the active site of Δ5Txl-2 interact with tubulin sulfhydryl groups, therefore playing a critical role as a regulator of MT stability and maintenance. Moreover, because Δ5Txl-2 has four additional structural cysteines it is plausible that disulfide bonding involving any of these residues could play a role in the binding mechanism. Studies are in progress to analyze the kinetics of Δ5Txl-2 binding to tubulin.

Txl-2/Δ5Txl-2 has an RCC1 signature in its C-terminal NDP kinase domain, a motif that is not present in any other member of the nm23 or thioredoxin family. RCC1 is a chromatin-bound guanine nucleotide exchange factor for the small nuclear GTPase Ran, a Ras-related protein (41). RCC1 has been implicated in nuclear cytoplasmic transport, mitotic spindle nucleation, and nuclear membrane formation (42). Interestingly, both a somatic and a testis-specific form of Ran have been described in mammals (43, 44). The testis-specific variant of Ran is found in the spermatid manchette, a location where RCC1 has also been found (42, 44). The spermatid manchette is a transient microtubular structure that develops during spermiogenesis and caudally surrounds the spermatid nucleus (45). The manchette has been proposed recently to be a transient storage location for both signaling and structural proteins involved in nucleocytoplasmatic trafficking or eventually sorted to the centrosome and the developing spermatid tail (32, 46). This sorting mechanism has been named intramanchette

transport, in close reference to the so-called intraflagellar transport (46, 47). Both intramanchette and intraflagellar transport involve molecular motors (primarily kinesins and dyneins) mobilizing a multicomplex protein raft to which cargo proteins or precursors for the assembly of the axoneme of a flagellum or a cilium are bound and transported to the tip of the axoneme (46). Thus, the potential association of Txl-2/Δ5Txl-2 with Ran by its RCC1 motif may be an indirect mechanism of binding to MTs.

As Txl-2 is also expressed in lung cilia the potential interacting proteins or substrates are not likely to be testis-specific but rather common to the microtubular infrastructure. The fact that Txl-2 contains thioredoxin and NDP kinase domains, both thought to be catalytic domains, in addition to its low abundance suggests that Txl-2 is more likely to act as a signaling/enzymatic protein rather than to have a structural role. The acquisition of a thioredoxin domain in flagellar proteins occurs early in evolution and is most likely a consequence of molecular or enzymatic requirements for a specific function in flagellum movement (11). In this context, it has been reported recently that the two thioredoxin domain-containing proteins from *Chlamydomonas* flagella, DLC14 and DLC15 (11), might regulate, by a redox mechanism, the ATPase activity of the flagella outer dynein arm (48). In addition, *Chlamydomonas* flagella p72 and sea urchin sperm axoneme IC1 proteins have been reported to have NDP kinase activity and suggested to be suppliers of the GTP for MT assembly (49). Interestingly, an exhaustive proteomic analysis of human ciliary proteins has found nm23-H5, nm23-H7, and Txl-2 as the only members of the NDP kinase family expressed in human axonemal extracts, adding further support to our data here reported on axonemal localization of Txl-2 (50). Based on this, a model could be proposed in which Txl-2 is responsible for GTP generation in cilia and flagella axoneme in these organisms. Furthermore, the presence of an RCC1 signature in Txl-2 suggests that it could interact with Ran and supply the GTP required for its enzymatic activity. Thus, it may be anticipated that disruption of a Ran-RCC1-Txl-2 pathway might lead to an alteration in the normal development of spermatozoa and other phenotypes associated with defective cilia physiology. Txl-2 expressed in bacteria is inactive in both the thioredoxin assay and the autophosphorylation assay. A similar situation was found for the closest Txl-2 homolog, Sptrx-2, as well as other thioredoxins and NDP kinases (12, 14, 20). Taken together, the lack of enzymatic activity of bacterially produced Txl-2, despite its interaction with thioredoxin reductase, indicates that post-translational modifications that might expose the active site upon conformational changes as well as interaction with other proteins or additional cofactors (cell- or tissue-specific) might be required for Txl-2 to function. Alternatively, because Txl-2 binds to MTs, the weak interaction detected *in vitro* with thioredoxin reductase may become physiologically significant *in vivo*.

The prominent expression of Txl-2 in microtubular structures in lung and testis may make it a candidate gene for diseases such as primary ciliary dyskinesia (PCD), an autosomal recessive disorder (OMIM 242650) characterized by a failure of proper ciliary and flagellar movement whose clinical manifestations are chronic respiratory infections, male infertility, and *situs inversus* (51, 52). The motility of cilia and flagella is generated in the axoneme, which has been estimated to be composed of more than 250 polypeptides (53). The axoneme consists of a core of nine peripheral + two central MT doublets connected by outer and inner dynein arms (composed of heavy, intermediate, and light chains) plus other accessory

proteins. Electron microscopy studies of the sperm of patients affected by PCD reveal multiple phenotypes with anomalies in both MT and dynein arm organization, indicating that this is a genetically highly heterogeneous disease (51). To determine whether any breakpoint in the region where the human Txl-2 gene maps has been reported to be associated with any of the PCD phenotypes, we screened the Mendelian Cytogenetics Network Data base (www.wjc.ku.dk/databases) and found one translocation (46, XY, t (3, 8) (q23;p23)) with an associated trait of azoospermia/oligospermia. Interestingly, two more breakpoints in the Txl-2 region are associated with hydrocephalus, a phenotype that is assumed to be a consequence of malfunctioning of the cilia of ependymal cells that facilitate circulation of the cerebral spinal fluid (54).

In summary, we have identified and characterized a new protein composed of thioredoxin and NDP kinase domains which binds directly to MTs. Its axonemal localization in sperm flagella and lung cilia indicates that it is a component of the axonemal machinery taking part in regulation of ciliary and flagellar movement and that Txl-2 is a potential susceptibility candidate gene involved in the PCD phenotype.

Supplementary Material

Refer to Web version on PubMed Central for supplementary material.

Acknowledgments

We thank Prof. Niels Tommerup for invaluable help with the Mendelian Cytogenetic Network data base and Dr. Elias S. J. Arnér for critical reading of the manuscript and helpful suggestions.

References

1. Arner ES, Holmgren A. Eur J Biochem. 2000; 267:6102–6109. [PubMed: 11012661]
2. Tanaka T, Nakamura H, Nishiyama A, Hosoi F, Masutani H, Wada H, Yodoi J. Free Radic Res. 2000; 33:851–855. [PubMed: 11237106]
3. Powis G, Montfort WR. Annu Rev Pharmacol Toxicol. 2001; 41:261–295. [PubMed: 11264458]
4. Eklund H, Gleason FK, Holmgren A. Proteins Struct Funct Genet. 1991; 11:13–28. [PubMed: 1961698]
5. Laurent TC, Moore EC, Reichard P. J Biol Chem. 1964; 239:3436–3444. [PubMed: 14245400]
6. Gan ZR. J Biol Chem. 1991; 266:1692–1696. [PubMed: 1988444]
7. Pedrajas JR, Kosmidou E, Miranda-Vizuete A, Gustafsson J-Å, Wright APH, Spyrou G. J Biol Chem. 1999; 274:6366–6373. [PubMed: 10037727]
8. Wollman E, d'Auriol L, Rimsky L, Shaw A, Jacquot J, Wingfield P, Graber P, Dessarps F, Robin P, Galibert F, Bertoglio J, Fradelizi P. J Biol Chem. 1988; 263:15506–15512. [PubMed: 3170595]
9. Spyrou G, Enmark E, Miranda-Vizuete A, Gustafsson J-Å. J Biol Chem. 1997; 272:2936–2941. [PubMed: 9006939]
10. Miranda-Vizuete A, Damdimopoulos AE, Gustafsson JA, Spyrou G. J Biol Chem. 1997; 272:30841–30847. [PubMed: 9388228]
11. Patel-King RS, Benashski SE, Harrison A, King SM. J Biol Chem. 1996; 271:6283–6291. [PubMed: 8626422]
12. Miranda-Vizuete A, Gustafsson J-Å, Spyrou G. Biochem Bio-phys Res Commun. 1998; 243:284–288.
13. Miranda-Vizuete A, Ljung J, Damdimopoulos AE, Gustafsson JA, Oko R, Pelto-Huikko M, Spyrou G. J Biol Chem. 2001; 276:31567–31574. [PubMed: 11399755]

14. Sadek CM, Damdimopoulos AE, Pelto-Huikko M, Gustafsson JJ, Spyrou G, Miranda-Vizuete A. Genes Cells. 2001; 6:1077–1090. [PubMed: 11737268]
15. Ogawa K, Takai H, Ogiwara A, Yokota E, Shimizu T, Inaba K, Mohri H. Mol Biol Cell. 1996; 7:1895–1907. [PubMed: 8970153]
16. Postel EH. Int J Biochem Cell Biol. 1998; 30:1291–1295. [PubMed: 9924799]
17. Lombardi D, Lacombe ML, Paggi MG. J Cell Physiol. 2000; 182:144–149. [PubMed: 10623877]
18. Hartsough MT, Steeg PS. J Bioenerg Biomembr. 2000; 32:301–308. [PubMed: 11768314]
19. Lacombe ML, Milon L, Munier A, Mehus JG, Lambeth DO. J Bioenerg Biomembr. 2000; 32:247–258. [PubMed: 11768308]
20. Munier A, Feral C, Milon L, Pinon VP, Gyapay G, Capeau J, Guellaen G, Lacombe ML. FEBS Lett. 1998; 434:289–294. [PubMed: 9742940]
21. Mehus JG, Deloukas P, Lambeth DO. Hum Genet. 1999; 104:454–459. [PubMed: 10453732]
22. Altschul SF, Koonin EV. Trends Biochem Sci. 1998; 23:444–447. [PubMed: 9852764]
23. Kussmann M, Nordhoff E, Rahbek-Nielsen H, Haebel S, Rossel-Larsen M, Jakobsen L, Gobom J, Mirgorodskaya E, Kroll-Kristensen A, Palm L, Roepstorff P. J Mass Spectrom. 1997; 32:593–601.
24. Oko R. Andrologia. 1998; 30:193–206. [PubMed: 9739416]
25. Oko RJ, Jando V, Wagner CL, Kistler WS, Hermo LS. Biol Reprod. 1996; 54:1141–1157. [PubMed: 8722637]
26. Leblond C, Clermont Y. Am J Anat. 1952; 90:167–215. [PubMed: 14923625]
27. Junco A, Bhullar B, Tarnasky HA, van der Hoorn FA. Biol Reprod. 2001; 64:1320–1330. [PubMed: 11319135]
28. Bairoch A, Buchner P, Hofmann K. Nucleic Acids Res. 1997; 25:217–221. [PubMed: 9016539]
29. Lecroisey A, Lascu I, Bominaar A, Veron M, Delepierre M. Biochemistry. 1995; 34:12445–12450. [PubMed: 7547990]
30. Biondi RM, Engel M, Sauane M, Welter C, Issinger OG, Jimenez de Asua L, Passeron S. FEBS Lett. 1996; 399:183–187. [PubMed: 8980148]
31. Milon L, Meyer P, Chiadmi M, Munier A, Johansson M, Karlsson A, Lascu I, Capeau J, Janin J, Lacombe ML. J Biol Chem. 2000; 275:14264–14272. [PubMed: 10799505]
32. Kierszenbaum AL. Mol Reprod Dev. 2001; 59:347–349. [PubMed: 11468770]
33. Valiron O, Caudron N, Job D. Cell Mol Life Sci. 2001; 58:2069–2084. [PubMed: 11814057]
34. Roymans D, Vissenberg K, De Jonghe C, Willems R, Engler G, Kimura N, Grobben B, Claes P, Verbelen JP, Van Broeckhoven C, Slegers H. Exp Cell Res. 2001; 262:145–153. [PubMed: 11139339]
35. Pinon VP, Millot G, Munier A, Vassy J, Linares-Cruz G, Capeau J, Calvo F, Lacombe ML. Exp Cell Res. 1999; 246:355–367. [PubMed: 9925751]
36. Gervasi F, D'Agnano I, Vossio S, Zupi G, Sacchi A, Lombardi D. Cell Growth Differ. 1996; 7:1689–1695. [PubMed: 8959337]
37. Lombardi D, Sacchi A, D'Agostino G, Tibursi G. Exp Cell Res. 1995; 217:267–271. [PubMed: 7698225]
38. Nickerson JA, Wells WW. J Biol Chem. 1984; 259:11297–11304. [PubMed: 6088539]
39. Padma P, Hozumi A, Ogawa K, Inaba K. Gene (Amst). 2001; 275:177–183. [PubMed: 11574167]
40. Chaudhuri AR, Khan IA, Luduena RF. Biochemistry. 2001; 40:8834–8841. [PubMed: 11467944]
41. Moore JD. Bioessays. 2001; 23:77–85. [PubMed: 11135312]
42. Zou Y, Millette CF, Sperry AO. Biol Reprod. 2002; 66:843–855. [PubMed: 11870094]
43. Coutavas EE, Hsieh CM, Ren M, Drivas GT, Rush MG, D'Eustachio PD. Mamm Genome. 1994; 5:623–628. [PubMed: 7849398]
44. Kierszenbaum AL, Gil M, Rivkin E, Tres LL. Mol Reprod Dev. 2002; 63:131–140. [PubMed: 12211070]
45. Mochida K, Tres LL, Kierszenbaum AL. Dev Biol. 1998; 200:46–56. [PubMed: 9698455]
46. Kierszenbaum AL. Mol Reprod Dev. 2002; 63:1–4. [PubMed: 12211054]
47. Rosenbaum JL, Cole DG, Diener DR. J Cell Biol. 1999; 144:385–388. [PubMed: 9971734]

48. Harrison A, Sakato M, Tedford HW, Benashski SE, Patel-King RS, King SM. Cell Motil Cytoskeleton. 2002; 52:131–143. [PubMed: 12112141]

49. Patel-King RS, Benashski SE, King SM. J Biol Chem. 2002; 277:34271–34279. [PubMed: 12095989]

50. Ostrowski LE, Blackburn K, Radde KM, Moyer MB, Schlatzer DM, Moseley A, Boucher RC. Mol Cell Proteomics. 2002; 1:451–465. [PubMed: 12169685]

51. Blouin JL, Meeks M, Radhakrishna U, Sainsbury A, Gehring C, Sail GD, Bartoloni L, Dombi V, O'Rawe A, Walne A, Chung E, Afzelius BA, Armengot M, Jorissen M, Schidlow DV, van Maldergem L, Walt H, Gardiner RM, Probst D, Guerne PA, Delozier-Blanchet CD, Antonarakis SE. Eur J Hum Genet. 2000; 8:109–118. [PubMed: 10757642]

52. Cowan MJ, Gladwin MT, Shelhamer JH. Am J Med Sci. 2001; 321:3–10. [PubMed: 11202477]

53. Dutcher SK. Trends Genet. 1995; 11:398–404. [PubMed: 7482766]

54. Sapiro R, Kostetskii I, Olds-Clarke P, Gerton GL, Radice GL, Strauss IJ. Mol Cell Biol. 2002; 22:6298–6305. [PubMed: 12167721]

55. Hanks SK, Quinn AM, Hunter T. Science. 1988; 241:42–52. [PubMed: 3291115]

56. Kong A, Gudbjartsson DF, Sainz J, Jonsdottir GM, Gudjonsson SA, Richardsson B, Sigurdardottir S, Barnard J, Hallbeck B, Masson G, Shlien A, Palsson ST, Frigge ML, Thorgeirsson TE, Gulcher JR, Stefansson K. Nat Genet. 2002; 31:241–247. [PubMed: 12053178]

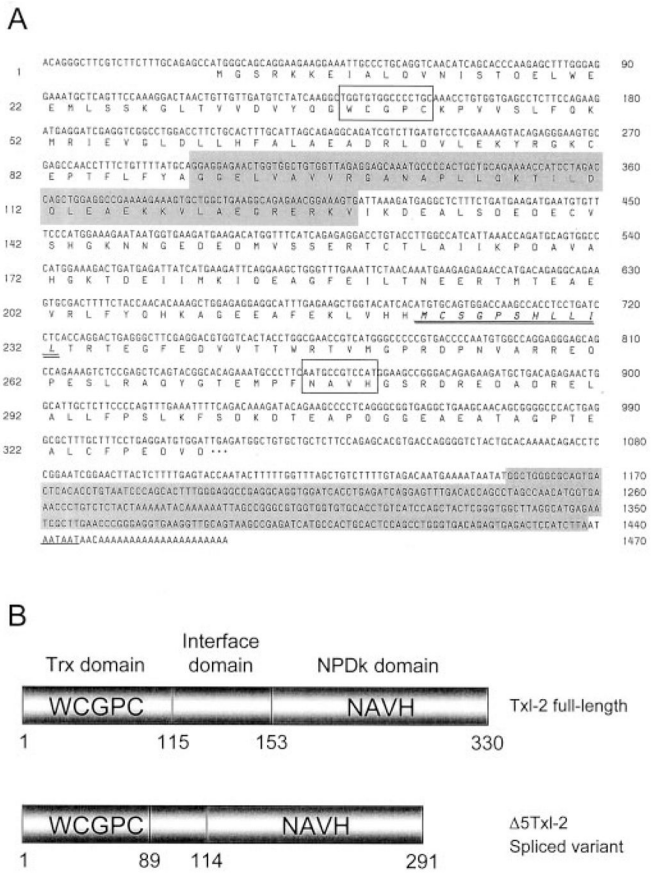

Fig. 1. Nucleotide/protein sequence analysis and protein domain organization of human Txl-2

A, nucleotide and amino acid sequence of human Txl-2 gene and protein. *Numbers* on the *left* indicate amino acids, and on the *right* they indicate nucleotides. Thioredoxin and NDP kinase active sites are *boxed*. The RCC1 signature is *double underlined*, and the potential polyadenylation signal in the 3′-UTR is *underlined*. Exon 5 (absent in the Δ5Txl-2 variant) within the ORF and the short interspersed repetitive element repeat within the 3′-UTR are *shadowed*. *B*, domain organization of Txl-2 and Δ5Txl-2 proteins. *Numbers* indicate the amino acids flanking the thioredoxin, interface, and NDP kinase domains.

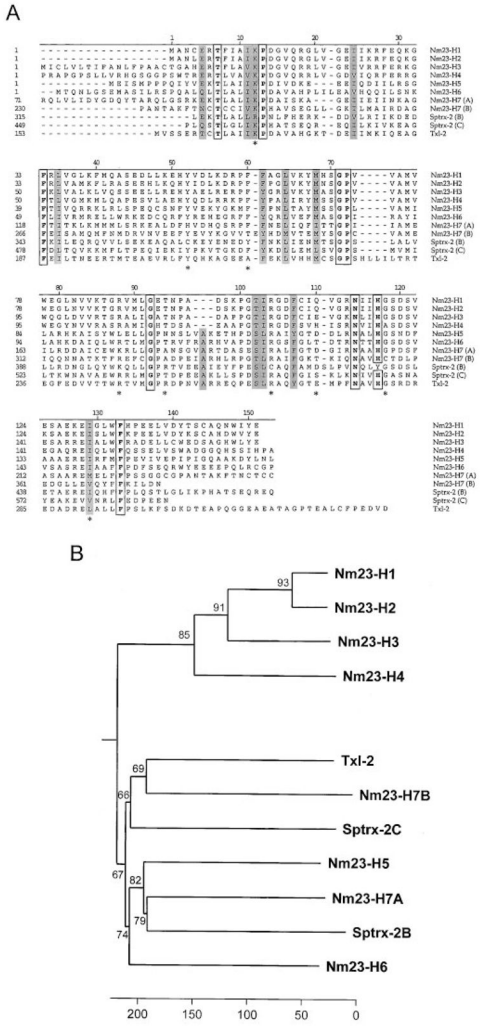

Fig. 2. Homology alignment and phylogenetic analysis of human Txl-2 with all the members of the NDP kinase family of proteins

A, primary sequence comparison of the NDP kinase domains of the human nm23/NDP kinase proteins. The *numbering* at the *top* refers to the nm23-H1 sequence; *numbers* on the *left* indicate the amino acid residue for each respective full-length protein. Identical (*empty boxes*) and conserved (*gray boxes*, according to Ref. 55) residues within all sequences are indicated. The *asterisk* denotes residues involved in catalysis and stability (19). Note the amino acid insertion in Txl-2 where the RCC1 signature (MCSGPSHLLIL) is located. *B*, phylogenetic tree of human NDP kinases. The *scale* indicates the number of substitution events/100 bases. The percentage bootstrap values (based on 1,000 replications) are given on the *nodes* of the *tree*.

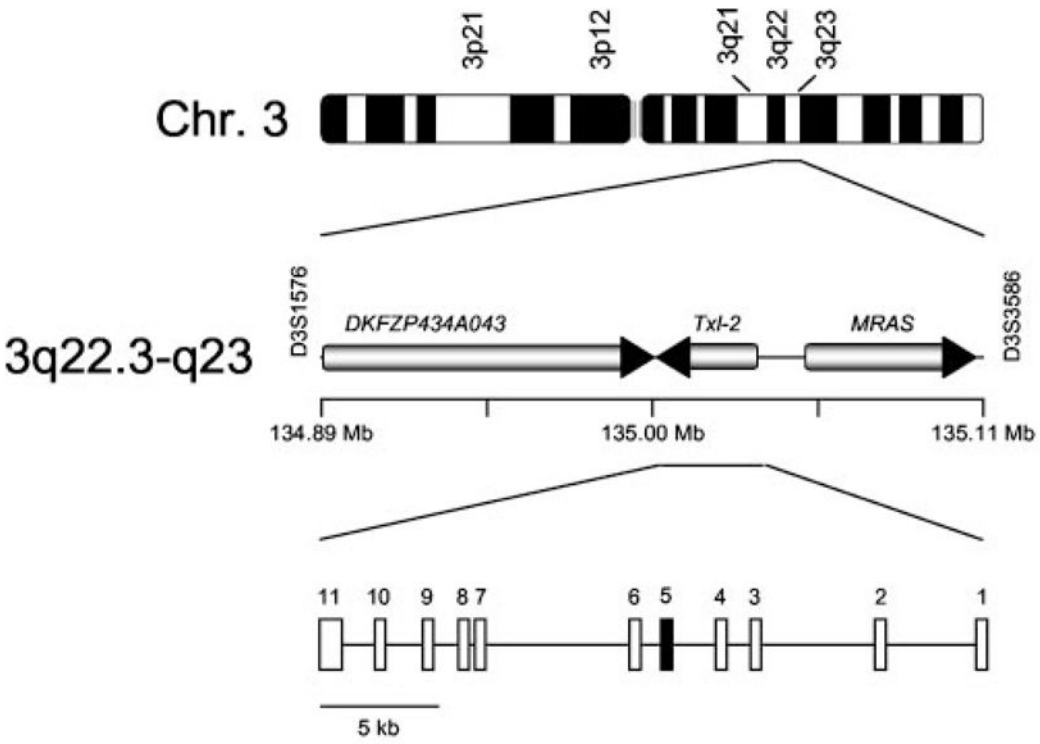

Fig. 3. Chromosomal localization and genomic organization of human Txl-2 gene

The human Txl-2 gene is located between the markers D3S1576 and D3S3586 at 144.46–145.33 cM from the top of the linkage group of human chromosome 3 (based on deCODE high resolution recombination map of human genome; see Ref. 56). By comparing this location with other genes in the region we have mapped Txl-2 gene to 3q22.3-q23 flanked by the genes *DKFZP434A043* and *MRAS*. The human Txl-2 gene is organized in 11 exons, and exon 5 (*black*) is absent in the Δ5Txl-2 variant.

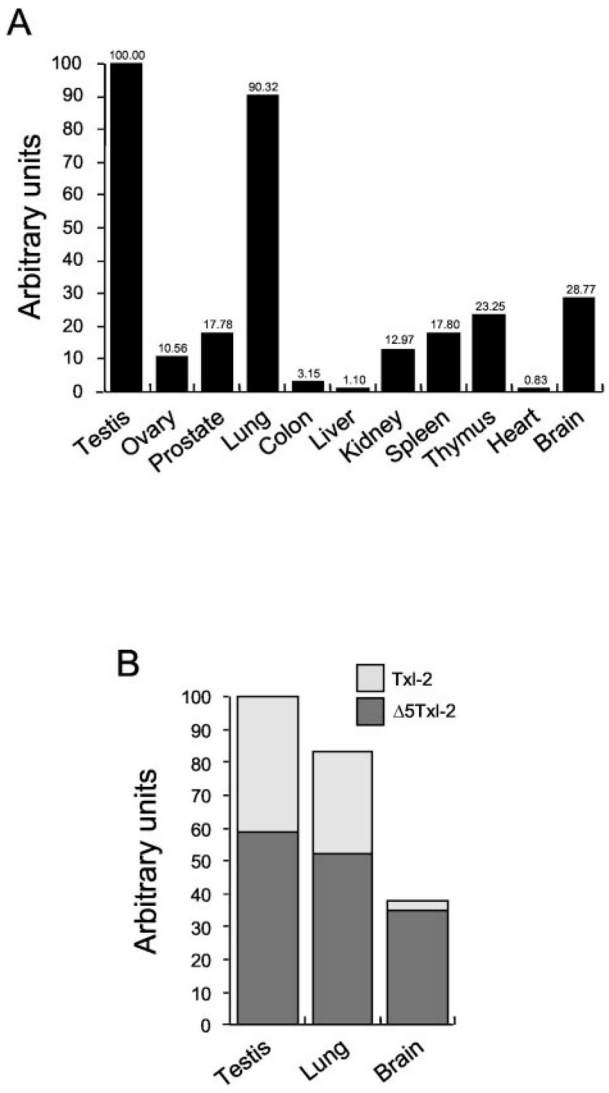

Fig. 4. Relative expression of Txl-2 mRNA in human tissues

Real time PCR was used to quantify Txl-2 mRNA using the standard curve method. Values were normalized to GAPDH. *A*, *bars* represent the mean amount of total Txl-2 mRNA for each tissue as determined in triplicate samples. *B*, real time PCR was used to determine the relative amounts of full-length and alternatively spliced Δ5Txl-2 in human testis, lung, and brain. All experiments were performed in triplicate, and similar results were obtained in at least three separate experiments. The value for testis was set as 100.

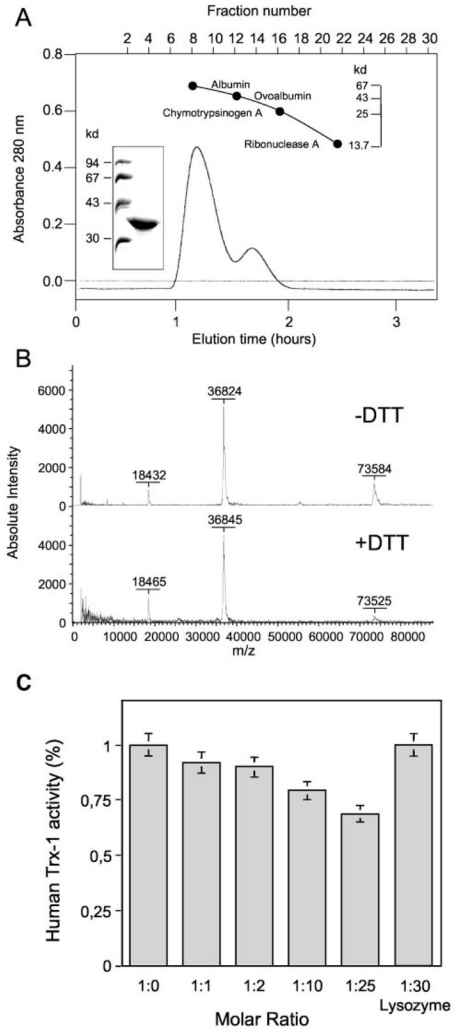

Fig. 5. Biochemical characterization of recombinant human Txl-2

A, gel filtration chromatography of human Txl-2. Elution profile of human Txl-2 applied to a Superdex 75 column in a volume of 5 ml, at a final concentration of 2 mg/ml, and a flow rate of 5 ml/cm^2/h. The *inset* shows the SDS-PAGE on the fractions eluted from the Superdex 75 column demonstrating the integrity of Txl-2. *B*, MALDI-TOF analysis of human Txl-2. The spectrum shows the single and double charged ions as well as the dimeric form of Txl-2. A decrease in the dimeric form is obtained upon incubation with DTT. *C*, dominant negative activity of human Txl-2. The dominant negative effect of full-length Txl-2 on Trx-1 enzymatic activity was carried out in the presence of NADPH and thioredoxin reductase. The assay conditions were identical to those described previously (13) except that increasing amounts of Txl-2 protein were added to the mix prior to initiating the reaction. Lysozyme was used as a control at the highest molar ratio. The reaction was initiated by adding 5 μl of calf thymus thioredoxin reductase (50 A_{412} units) and stopped after 20 min by the addition of 6 M guanidine HCl and 1 mM 5,5′-dithiobis(nitrobenzoic acid). The experiment was repeated three times.

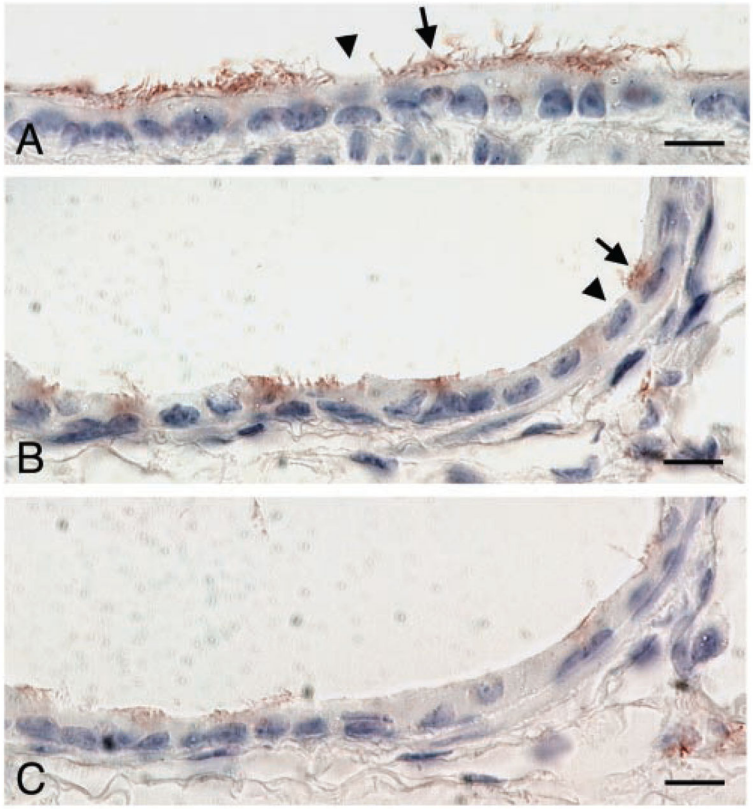

Fig. 6. Immunohistochemical localization of Txl-2 protein in lung

Paraffin sections of mouse lung were immunoperoxidase stained with affinity-purified anti-Txl-2 antibodies diluted 1/20. *A*, large intrapulmonary airway; *B*, small intrapulmonary airway. Both locations exhibit clear immunostaining specifically localized to the cilia of ciliated epithelial cells (*arrows*). No staining is observed in nonciliated epithelial cells (*arrowheads*). *C*, immunoreactivity is reduced substantially when Txl-2-blocking peptide is included with the primary antibody. *Bar*, 10 μm.

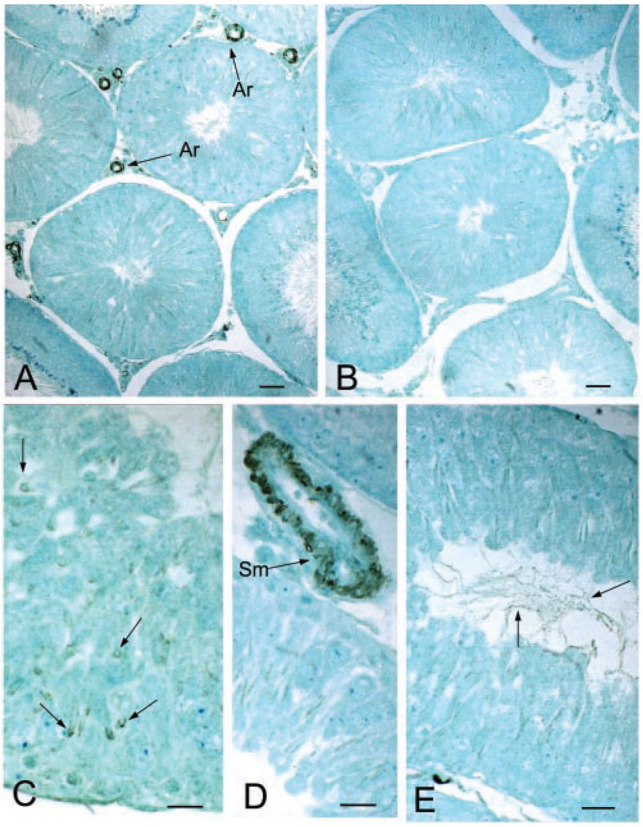

Fig. 7. Immunohistochemical localization of Txl-2 protein in testis

Paraffin sections of rat seminiferous tubules were immunoperoxidase stained with affinity-purified anti-Txl-2 antibodies diluted 1/100. *A*, survey section showing obvious immunostaining of the arterioles (*Ar*). *B*, no immunoreactivity is detectable when anti-Txl-2 is preincubated with human recombinant Txl-2. *C*, at higher magnification, during the spermatid elongation phase (steps 8–14), immuno-staining was apparent at the periphery of the spermatid nucleus and beyond (*arrows*), suggesting labeling of the microtubular manchette. *D*, at this magnification it is clear that the smooth muscle (*Sm*) wall of the arteriole is immunoreactive. *E*, fainter immunostaining of the sperm tails (*arrows*) in the lumen is also apparent. *Bar*, 10 μm.

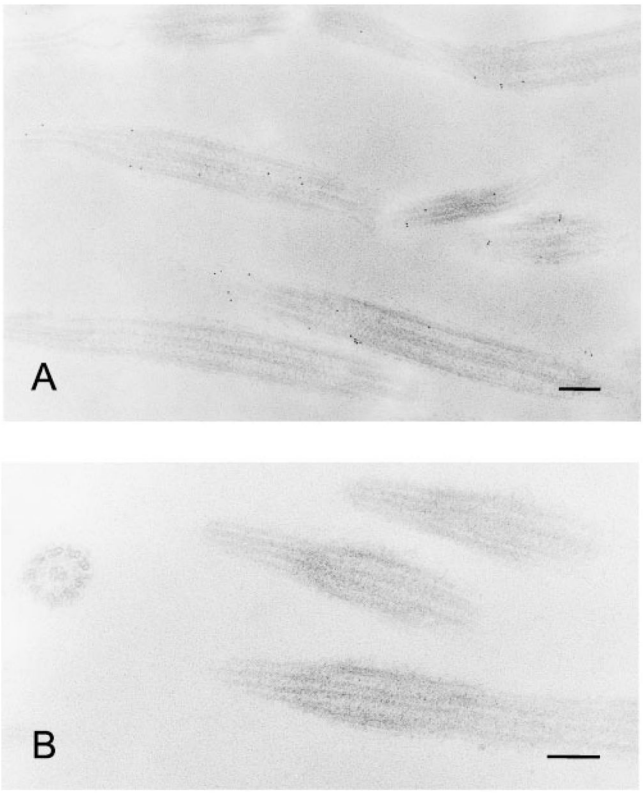

Fig. 8. Immunogold electron microscopy localization of Txl-2 protein in lung

A, electron micrographs of sections through mouse lung ciliated epithelium immunogold labeled with anti-Txl-2. Labeling is found in close association with the MTs of the axoneme. *B*, mouse cilia labeled with anti-Txl-2 preincubated with human recombinant Txl-2. No immunogold labeling of the MTs of the axoneme is evident. *Bar*, 0.2 μm.

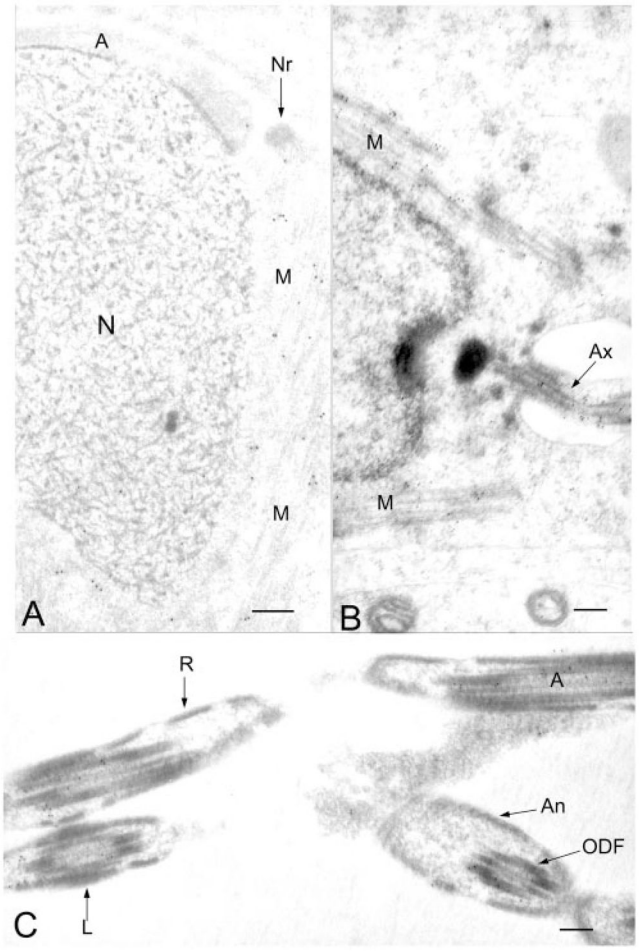

Fig. 9. Immunogold electron microscopy localization of Txl-2 protein in spermatids

Shown are electron micrographs of sections through spermatid heads and tails immunogold labeled with anti-Txl-2. *A*, elongating spermatid in step 10 showing labeling of the microtubular manchette (*M*). Abbreviations: *A*, acrosome; *Nr*, nuclear ring of the manchette; *N*, nucleus. *B*, spermatid in step 12 showing labeling of the manchette and of the axoneme (*Ax*) *C*, spermatid tails in step 15 showing labeling of the axoneme. *R* and *L*, ribs and longitudinal columns of the fibrous sheath; *An*, anlagen of the fibrous sheath, *ODF*, outer dense fibers. *Bar*, 0.2 μm.

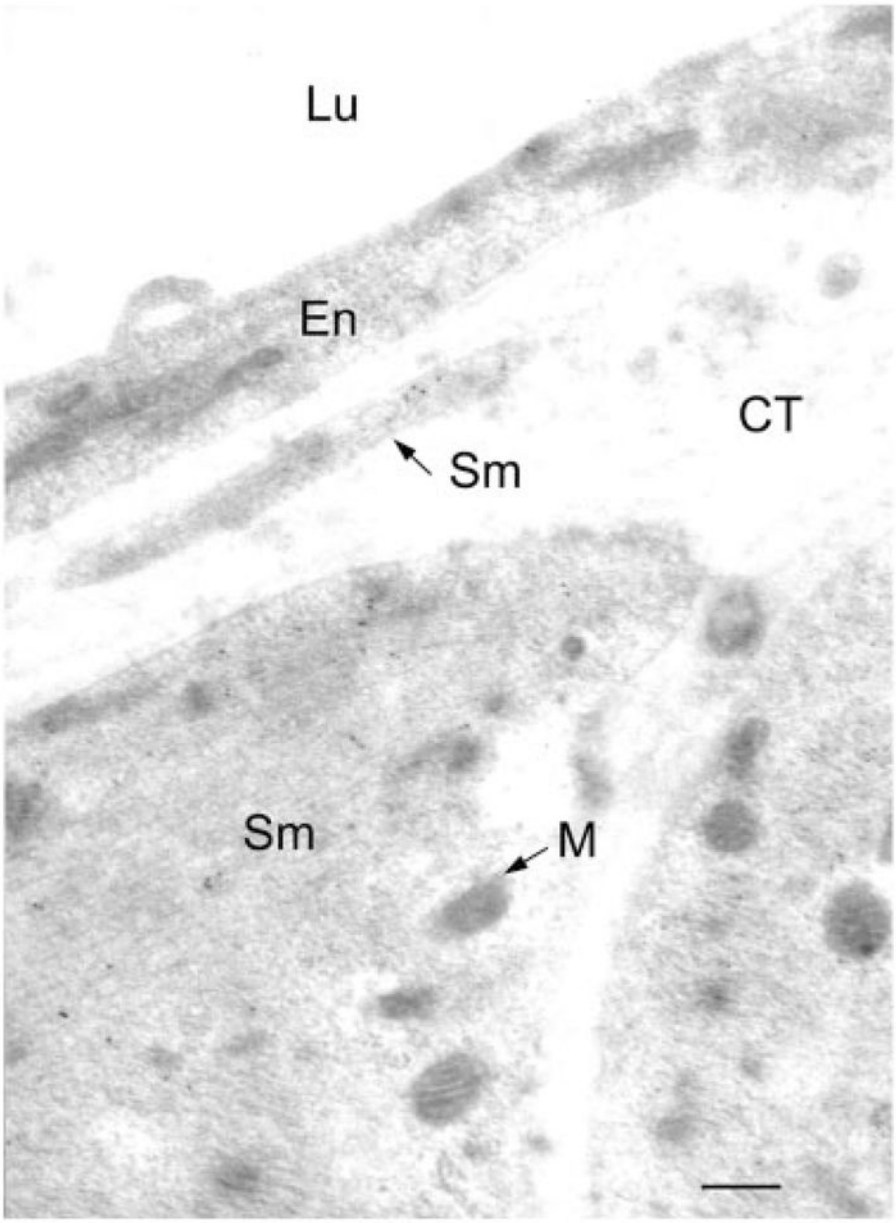

Fig. 10. Immunogold electron microscopy localization of Txl-2 protein in testicular arterioles

The testicular arteriole wall shows immunoreactivity in smooth muscle (*Sm*) cell. In contrast, the endothelium (*En*) does not appear to be immunogold labeled. *CT*, connective tissue; *M*, mitochondria; *Lu*, lumen. *Bar*, 0.2 μm.

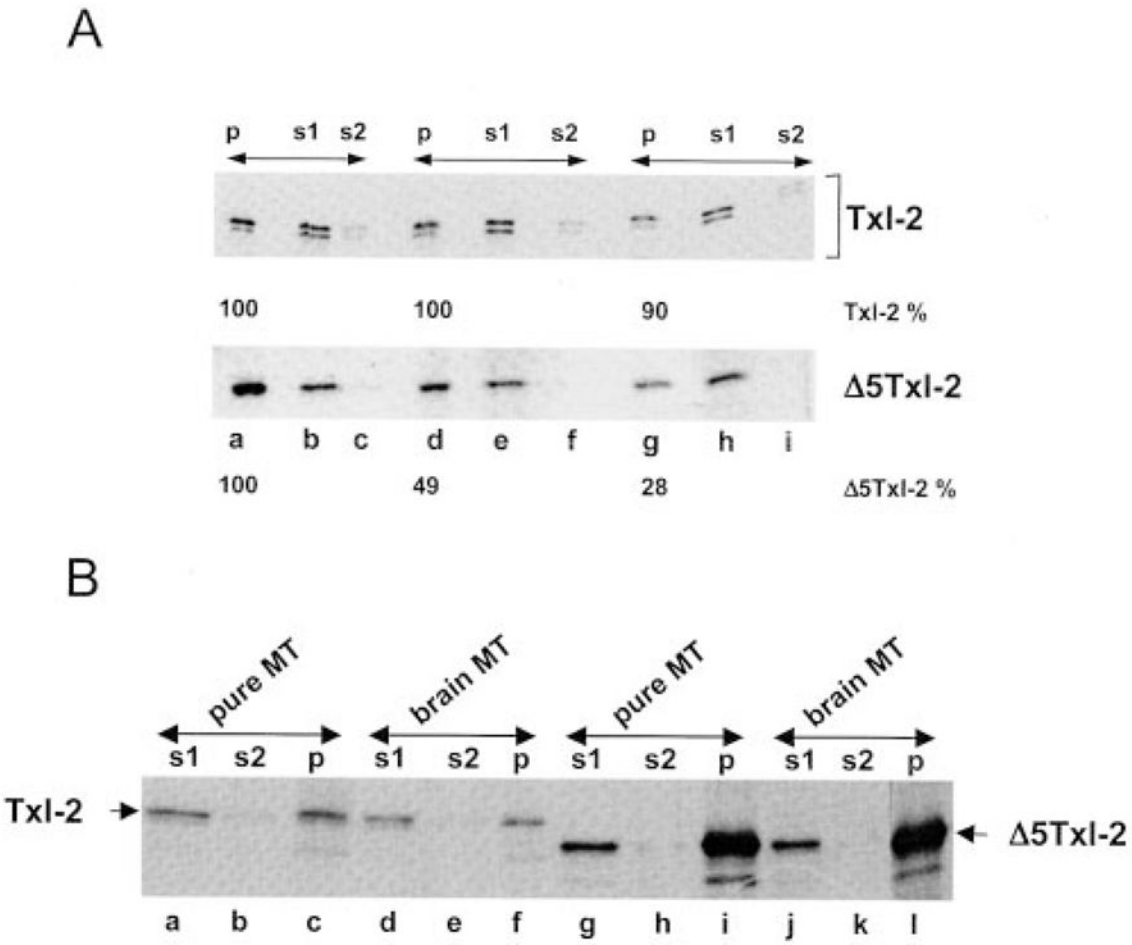

Fig. 11. Txl-2 and Δ5Txl-2 bind MTs *in vitro* with differential affinity

A, ^{35}S-labeled Txl-2 and Δ5Txl-2 were synthesized by *in vitro* translation and incubated with rat brain MTs. Binding reactions were pelleted through a cushion, washed, and this procedure was repeated. Resulting supernatant 1 (*s1*), supernatant 2 (*s2*) and MT pellets (*p*) were analyzed for Txl-2 and Δ 5Txl-2 protein by SDS-PAGE and autoradiography. *Upper panel*, Txl-2 binding experiments; and *lower panel*, Δ5Txl-2 binding experiments. *Lanes a–c*, proteins were incubated with brain MTs (*MT*). *Lanes d–f*, Txl-2 and Δ5Txl-2 proteins were analyzed for MT binding after preincubation of MTs with recombinant Txl-2 protein. *Lanes g–i*, Txl-2 and Δ5Txl-2 proteins were analyzed for MT binding after preincubation of MTs with anti-Txl-2 antibodies. Binding of Txl-2 and Δ5Txl-2 proteins relative to untreated samples (arbitrarily set at 100%) is indicated as percents. *B*, to distinguish direct from indirect MT binding, ^{35}S-labeled Txl-2 (*lanes a–f*) and Δ5Txl-2 (*lanes g–l*) were synthesized by *in vitro* translation and incubated with purified rat brain MTs (*brain MT*) or with pure MTs prepared by polymerization of pure tubulin (*pure MT*). Pelleted MTs were washed, and supernatants and pellets were analyzed as described for *A*. *s1*, supernatant 1; *s2*, supernatant 2; *p*, pellet. Note the strong binding of ΔTxl-2 to pure MTs.